

***Ab initio* investigation of the first-order liquid-liquid phase transition in molten sulfur**

Ziqing Yang, Jiaxin Xu, Gang Zhao, and Dehua Wang

School of Physics and Optoelectronic Engineering, Ludong University, Yantai 264025, People's Republic of China (Received 7 October 2023; revised 28 November 2023; accepted 3 January 2024; published 16 January 2024)

Ab initio molecular dynamics simulations are used to investigate the first-order liquid-liquid phase transition (LLPT) in molten sulfur recently observed in experiments [Henry *et al.*, *Nature (London)* **584**, 382 (2020)]. Our calculated pair correlation functions are in good agreement with the experimental results, and our simulations capture the structural change from low-density liquid (LDL) to high-density liquid (HDL). By studying the microstructure, it is found that this structural change is in fact one between two polymer phases with different degrees of order, with HDL having a higher degree of order than LDL. There are more S_8 diradical structures in the long chain of LDL, but less in the long chain of HDL. This structural change may be related to the self-organized behavior of long-chain molecules in molten sulfur. However, no discontinuous change in density is found along the simulated isotherms, that is, the structural change based on *ab initio* calculations is continuous but not a first-order LLPT.

DOI: [10.1103/PhysRevB.109.014209](https://doi.org/10.1103/PhysRevB.109.014209)**I. INTRODUCTION**

The phenomenon of first-order phase transitions in liquids has attracted a great deal of public interest in recent decades. Traditionally, it has been widely believed that the structure of a simple liquid varies continuously with temperature or pressure. However, as early as 1990, Brazhkin *et al.* [1] found that the nonmetallic-metallic transition in liquid Se exhibits some features of a first-order liquid-liquid phase transition (LLPT) and predicted the possible existence of a liquid-liquid critical point (LLCP). In 1992, Poole *et al.* [2] found more direct evidence for LLPT and LLCP in supercooled water when they studied its anomalous thermodynamic properties using computer simulations. They found that each of the pressure-volume isotherms at lower temperatures exhibits an inflection that increases in strength with decreasing temperature. The shape and temperature dependence of these inflections are similar to what would occur for isotherms if a critical point were approached in temperature from above. This critical point was called the “second critical point,” below which there coexist two phases with different densities and structures. Subsequently, extensive evidence for LLPT has been found not only in supercooled water [3] but also in other liquids such as Al_2O_3 - Y_2O_3 [4], carbon [5,6], phosphorus [7–9], triphenyl phosphite [10], arsenic sulfide [11–13], silicon [14–19], nitrogen [20], hydrogen [21–23], and B_2O_3 [24,25]. Brazhkin and co-workers [26,27] provided a systematic and detailed summary of the evidence for the possible existence of LLPT in many liquids under high pressure. Among these, only the LLPT in molten phosphorus has unambiguous experimental evidence [7,8]. Most of the other evidence comes from computer simulations [6,11–23] and some evidence is even controversial [28,29]. Therefore, the first-order LLPT remains a focus of research. In all cases where evidence for a first-order LLPT has been found, the boundary between the high-density liquid (HDL) and low-density liquid (LDL) on the pressure-temperature phase diagram has a negative slope,

except for molten carbon [6]. This is due to the fact that HDL typically exhibits a more disordered structure and higher entropy than LDL. Thus, the slope is negative according to the Clapeyron equation ($dP/dT = \Delta S/\Delta V$).

Molten sulfur has also been suggested as a potential candidate for the existence of LLPT. Under atmospheric pressure, the stable solids, α sulfur (below 368 K) and β sulfur (368–388 K), consist of S_8 molecules [30], whereas at high pressure and temperature, the stable phase becomes a polymeric solid composed of helical chains [31]. At ambient pressure, the melting of β sulfur occurs at 388 K and the S_8 molecular structure remains in molten sulfur. As the temperature increases to 432 K, the molecular liquid undergoes a so-called “ λ transition” where it polymerizes into chains or larger ring-like structures, whereas this transition is not a first-order phase transition [32]. For molten sulfur at high temperature and pressure (above 900 K and 5 GPa), while the breakage of the chain structure accompanied by the semiconductor-metal transition has been observed [33–35], there is insufficient evidence to determine whether this transition is a first-order phase transition.

Recently, Henry *et al.* [36] conducted combined *in situ* density, x-ray diffraction, and Raman scattering measurements of molten sulfur in the pressure region below 3 GPa and observed the discontinuous change in density along the isotherms below 1035 K. This suggests the existence of a first-order LLPT and an LLCP in molten sulfur. Interestingly, unlike the LLPT in other liquids [3,4,7,8,11–23], the boundary of LDL and HDL in their results has a positive slope, indicating that HDL has a lower entropy than LDL. Due to the lack of atomic-level information on the structure of LDL and HDL, they were only able to infer that HDL may contain more polymer components than LDL based on the variation of the pair correlation function, which can lead to a lower mixing entropy in HDL. At the same time, again based on pair correlation functions, they obtained that the conformational entropy of HDL is lower than that of LDL. This is in complete contrast to the results obtained in

other liquids [3,4,7,8,11–23]. Therefore, in order to clarify the experimental observations, it is necessary to study the microstructure of molten sulfur at the atomic scale.

The development of *ab initio* molecular dynamics simulations has made it possible to study the atomic structure of molten sulfur from a first-principles perspective. In the present work, by means of *ab initio* molecular dynamics simulations, we focus on investigating the structural changes of molten sulfur as a function of density along the isotherm, in the hope of obtaining some detailed microscopic structural information of molten sulfur and theoretically discovering the nature of the structural changes. The paper is organized as follows: in Sec. II we describe the methodology of our simulations, the results and the corresponding discussion are reported in Sec. III, and a short summary is given in Sec. IV.

II. CALCULATIONAL METHODS

Our density function theory (DFT) based simulations were performed by the Vienna *ab initio* simulation package (VASP) [37,38] together with projector augmented wave (PAW) potentials [39,40]. For the exchange correlation function, Perdew-Burke-Ernzerhof generalized gradient approximation (PBE-GGA) [41] and local density approximation (LDA) [42] were used, respectively. The pair correlation functions $g(r)$ based on two approximate methods are compared with the experimental measurements [43] in Fig. S1 of the Supplemental Material [44]. It can be observed that GGA overestimates the positions of the first three coordination shells, especially the third one, compared to LDA. The calculated pressures based on PBE-GGA and LDA under the same temperature and density conditions are also compared with the experimental values [45,46]. Here, we monitored the reported “external pressure” in VASP and added the kinetic energy contribution $\rho k_B T$ to obtain the thermodynamic pressure. The results are listed in Table S1 of the Supplemental Material [44]. GGA overestimates the calculated pressure, while LDA underestimates it. However, the LDA based values are closer to the experimental results, hence the use of LDA in the present work. It should be noted that in Table S1 of the Supplemental Material [44] the negative pressure (-0.1363 GPa) means the liquid at $T = 550$ K, $\rho = 1.70$ g/cm³ is stretched within the frame of LDA.

The simulated system consists of 192 sulfur atoms placed in a simple cubic box with periodic boundary conditions. We evaluate the effect of the size of the simulation box and the results are shown in Fig. S2 of the Supplemental Material [44]. It can be found that a system of 192 atoms is sufficient to give converged structural properties and calculated pressures within the allowed error margin. The electronic wave functions are expanded in the plane wave basis set with an energy cutoff of 380 eV, which is proved to be adequate for achieving converged pressure (see Fig. S3 of the Supplemental Material [44]); the Γ point is used to sample the supercell Brillouin zone. The canonical ensemble (*NVT*) is adopted with a Nosé thermostat for temperature control [47]. The Newton equations of motion are integrated using the Verlet algorithm with a time step of 2 fs for the ion motion. Three isotherms are simulated at 550, 740, and 950 K. The adopted initial atomic configuration is a random distribution

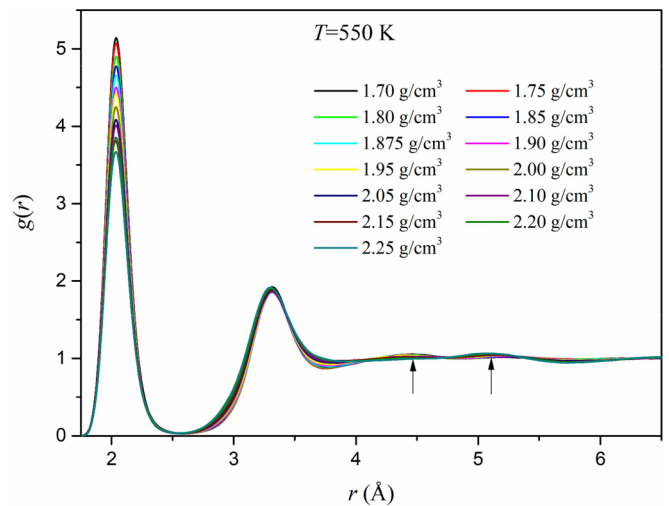


FIG. 1. The calculated $g(r)$ at different densities from 1.70 to 2.25 g/cm³ along the 550-K isotherm. The most noticeable position changes occur at the third and fourth peaks, located around 4.45 and 5.20 Å, respectively.

of 24 S_8 molecules in the supercell, followed by an initial equilibration run of 60 ps at 1100 K, after which the system is quenched to 550 K. A total of 13 state points with increasing densities ranging 1.70–2.25 g/cm³ were simulated along the 550-K isotherm. At each state point, molecular dynamics simulations are performed for at least 100 ps. For the 740-K isotherm simulations, the density is gradually reduced from 2.25 to 1.70 g/cm³. Simulations at 950 K isotherm are similar to those at 550 K.

III. RESULTS AND DISCUSSION

For comparison with experimental results, we first simulate 13 state points along the 550-K isotherm with densities ranging 1.70–2.25 g/cm³. Our calculated pair correlation functions $g(r)$ are shown in Fig. 1. It can be seen that the positions of the first and second peaks are almost constant with density, which is in agreement with experimental observation [36,48]. The most noticeable position changes occur at the third and fourth peaks, located around 4.45 and 5.20 Å, respectively. Their enlarged images and comparison with the experimental results are shown in Fig. 2. The location of the third peak in our results is in good agreement with the experimental observation under low temperature and low pressure [36,43,48,49], and the location of the fourth peak is also in good agreement with the experimental observation under high temperature and high pressure (900 K, 5.6 GPa) [33]. This implies that our calculated results above are plausible and capture the transition between these two structures. At low densities, the intensity of the third peak is significantly higher than that of the fourth peak. As the density increases, the intensity of the third peak gradually decreases and the position gradually shifts to the right until it becomes a shoulder. However, the intensity of the fourth peak gradually increases with density, its position gradually shifts to the left, and its height becomes significantly higher than that of the third peak at high densities. These results suggest

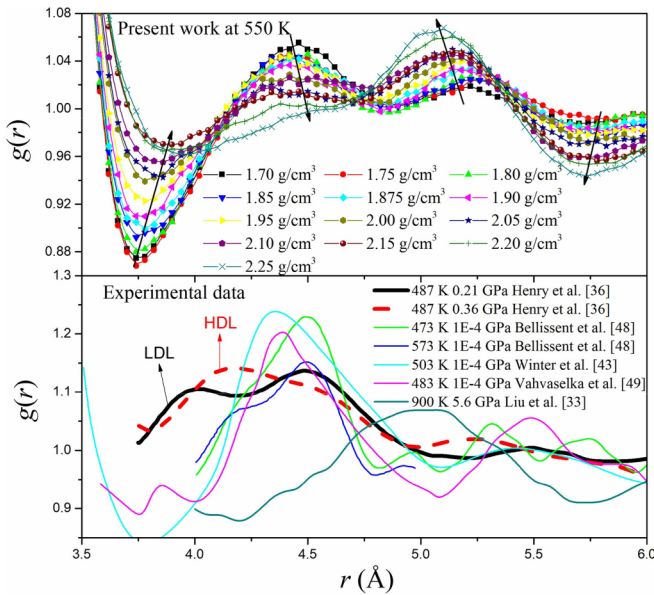


FIG. 2. Enlarged images of the third and fourth peaks in $g(r)$ at 550 K and comparison with the experimental results [33,36,43,48,49]. Our results qualitatively reproduce experimental observations. The direction of the arrow indicates an increase in density.

that the structural order of molten sulfur changes with increasing density. Considering that van der Waals interactions and noncovalent interactions may affect the third and fourth peaks of the $g(r)$, we also performed *ab initio* molecular dynamics based on the strongly constrained and appropriately normed (SCAN) functional [50,51], which satisfies all 17 known exact constraints on the semilocal exchange-correlation functional and is able to capture much of the intermediate-range part of the van der Waals interaction. The results are shown in Fig. S4 of the Supplemental Material [44]. The SCAN functional does capture the height of the third peak better than LDA, but the trend of the third and fourth peaks with density is the same in both cases.

In the experimental observation by Henry *et al.* [36], except for a peak at about 4.45 Å, another peak occurs at about 4.0 Å for LDL. As LDL transforms into HDL, the peak height at 4.45 Å becomes lower, while the peak height at 4.0 Å becomes higher and moves to 4.15 Å. As can be seen in Fig. 2, there is no such clear peak at 4.0 Å in the LDL of the other experiments [43,48,49], nor is it found in our work. However, it can be found that in our results the valley around 3.75 Å becomes shallower and shifts to the right with increasing density. In addition, it also can be found that, in $g(r)$ of Henry *et al.* [36], a peak at 5.5 Å in LDL is also shifted to the left to about 5.25 Å in HDL, in qualitative agreement with the change of the fourth peak in our results. Thus our results qualitatively reproduce the experimental results of Henry *et al.* [36]. Henry *et al.* suggest that the 4.45-Å peak is related to molecule content and the decrease of its height is due to reduced molecule content, while the variation in the 4.0-Å peak indicates that the polymer content in HDL is greater than in LDL. In Fig. 3 we show atomic snapshots at 1.70 and 2.25 g/cm^3 . It can be seen that almost no S_8 molecules

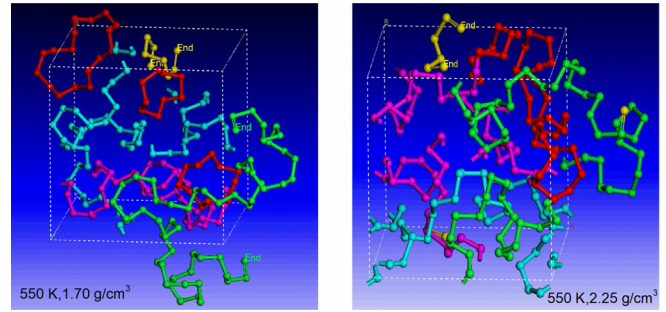


FIG. 3. Atomic snapshots at 1.70 and 2.25 g/cm^3 . One color represents a chain or a ring. The ends of finite-length atomic chains are marked with “End.” Almost no S_8 molecules are found even in LDL; instead many chains or larger ringlike structures can be found.

are found even in LDL; instead many chains or larger ringlike structures can be found. This suggests that LDL is also dominated by the polymeric component. Thus, the peak of 4.45 Å in $g(r)$ actually indicates that the S_8 diradical in the polymer still partially retains the structural characteristics of S_8 molecules. That is, the structural transition we captured is the one between two structurally distinct polymer phases. There are more S_8 diradical structures in the long chain of LDL, but less in the long chain of HDL.

In order to compare the degree of order between LDL and HDL, we calculate the two-body pair correlation excess entropy S_2 according to the following equation: $S_2 = -2\pi\rho \int_0^\infty \{g(r)\ln[g(r)] - [g(r) - 1]\}r^2 dr$. The excess entropy S_{ex} is the difference between the thermodynamic entropy of the system and that of the equivalent ideal gas, which is given as $S_{\text{ex}} = S_2 + S_3 + \dots$, where S_2 is the pair correlation entropy, S_3 is the triplet correlation entropy, and so on. Baranyai and Evans [52,53] have found that S_2 contributes at least 85% of S_{ex} at liquid densities and the difference between S_{ex} and S_2 is nearly constant over a wide range of densities. Such a constant shift of S_2 would simply translate into a constant shift of the data on the graph with respect to S_{ex} . So, in the present work, S_{ex} is approximated by S_2 and discussed. The results of our calculated S_2 at different densities on the 573-K isotherm are shown in Fig. 4. It can be seen that S_2 decreases with increasing density, suggesting that HDL is more ordered than LDL. This is in agreement with the experimental results of Henry *et al.* [36], i.e., the conformational entropy of HDL is lower than that of LDL.

Henry *et al.* found that this phase transition could not be observed at temperatures above 1035 K [36]. Here, to examine the effect of temperature on this structural change, we also performed simulations at two additional isotherms, 740 and 950 K. The results for the variation of the structure with density at these two temperatures are shown in Fig. 5. It can be seen that the structural changes due to density become less and less pronounced as the temperature increases. This is in general agreement with experimental observations. Figure 6 gives a snapshot of the atoms at 950 K. Comparing Fig. 3, it can be seen that at 550 K there are many infinite-length chains of atoms, which all become finite length at 950 K. Combining the above results, we speculate that this structural transition may be related to the self-organized behavior of

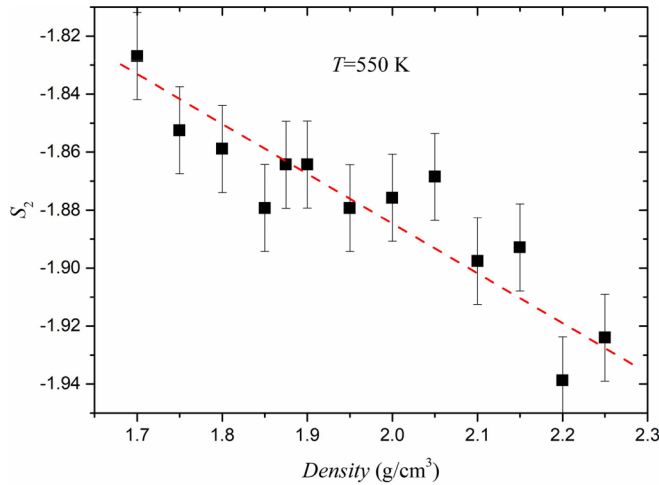


FIG. 4. Two-body excess entropy S_2^{ex} at different densities on the 550-K isotherm. It decreases with increasing density, suggesting that HDL is more ordered than LDL.

long-chain molecules. As the density increases, the atoms in the chain tend to be arranged in a more ordered manner in order to obtain a larger free volume, leading to a decrease in entropy. Upon increasing the temperature, this self-organized behavior becomes less pronounced due to the shortening of the long-chain molecules.

The pressure-density isotherms of Henry *et al.* [36] are replotted in Fig. 7(a), where the discontinuous changes in density are observed, which are direct evidence of a first-order LLPT. This discontinuous change in density disappears at temperatures greater than or equal to 1035 K, suggesting that the LLCP occurs at around 1035 K. In the present work, for comparison with experimental results, we also calculate the pressure as a function of density along the 550-K isotherm, which is shown in Fig. 7(b). At temperatures above 550 K and pressures below 3 GPa, there is a little experimental data available for comparison. Apart from the experimental results of Henry *et al.* [36], we only found those of Feher *et al.* [45]. In addition, Funakoshi and Nozawa [46] measured

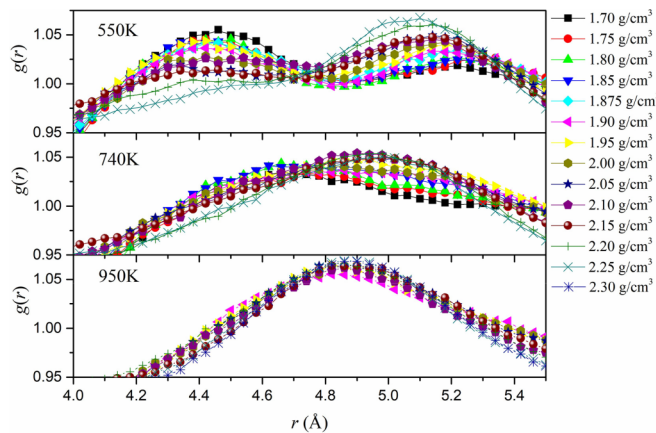


FIG. 5. The change of $g(r)$ with density at three temperatures. The structural changes become less and less pronounced as the temperature increases.

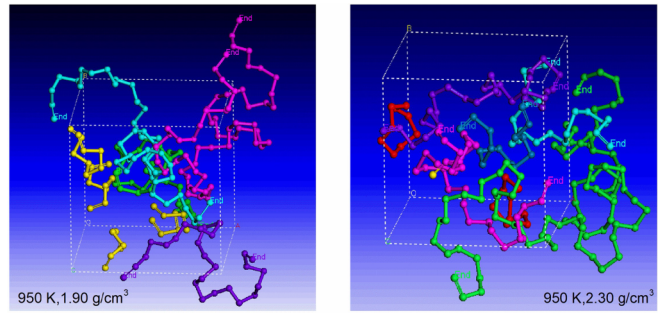


FIG. 6. Atomic snapshot of LDL and HDL at 950 K. One color represents a chain or a ring. The ends of finite-length atomic chains are marked with “End.”

the density of molten sulfur at high temperature (≥ 668 K) and high pressure (≥ 3 GPa). As can be seen in Fig. 7(b), although the pressure is underestimated by our simulations due to the limitations of the LDA itself, the trend of the variation of the pressure with density is generally consistent with the experimental results [36]. However, along the 550-K isotherm, we find no evidence for a first-order phase transition, that is, a discontinuous change in density. The SCAN functional overestimates the pressure, but no discontinuous change in density is observed in the curve either. In addition, we also simulate the 950-K isotherm [as shown in Fig. 7(c)], but still no discontinuous change in density is found. We suspect that this may be because the discontinuous change in density on these two isotherms is too small to be easily detected [see Fig. 7(a)]. In the results of Henry *et al.* [36], a larger discontinuous change in density is observed along the 740-K isothermal decompression curve. Such a large change makes the 740-K isotherm look very different from the other isotherms, as shown in Fig. 7(a). To test this scenario, we simulate the isothermal decompression curve at 740 K and the results are shown in Fig. 7(c). However, we still find no discontinuous density change. Using the GGA exchange correlation function, we do not find the discontinuous change in density either (not shown here). If the density-dependent pressures of LDL and HDL are fitted linearly, respectively, a crossover occurs at a density of about 1.985 g/cm^3 [see Fig. 7(b)], indicating a rapid structural change in the density range $1.90\text{--}2.05 \text{ g/cm}^3$, but not a first-order phase transition. This rapid structural change can also be observed from the changes in the third and fourth peaks of $g(r)$ in Fig. 7(d). When the density is lower than 1.95 g/cm^3 , the third peak is higher than the fourth one, meaning that the polymer component contains more S_8 diradical structures. However, the opposite is true for densities larger than 2.0 g/cm^3 .

We believe that the reason why no first-order phase transition is found in the simulations should not be due to the small number of atoms. In simulations of a first-order LLPT, even if it is not possible to reproduce the coexistence of the two phases on the isotherm with a small number of atoms, the isotherm usually exhibits van der Waals isotherm features, as in simulations of phosphorus [9], silicon [16,18], nitrogen [19], etc. However, the isotherms here also do not exhibit van der Waals isotherm features. Based on present results, we are unable to give a reason for the discrepancy between

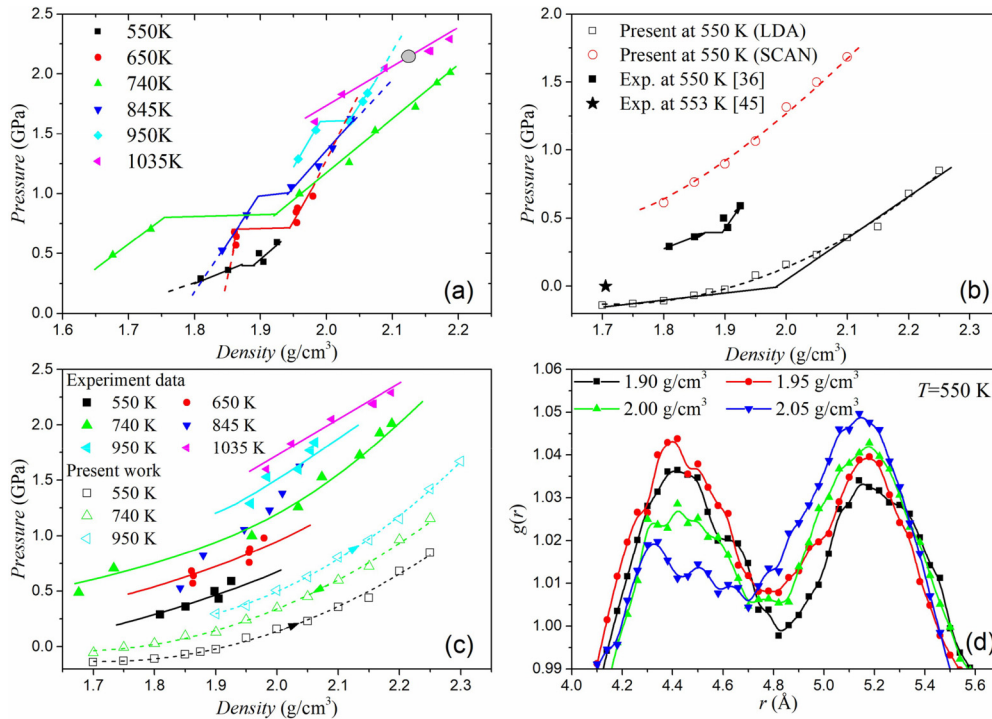


FIG. 7. (a) The replotted pressure-density isotherms of Henry *et al.* [36]. The discontinuous changes in density are direct evidence of a first-order LLPT. An LLCP (grey circle) occurs at around 1035 K. (b) The calculated pressure-density isotherm at 550 K is compared with experimental results [36,45]. The trend of the variation of the pressure with density is generally consistent with the experimental results. However, no evidence for a first-order phase transition is observed. (c) The calculated pressure-density isotherms at 550, 740, and 950 K are compared with experimental results [36]. The 740-K isotherm is decompression curve. No evidence for a first-order phase transition is observed in our simulations. (d) Enlarged images of the third and fourth peaks in $g(r)$ with the densities of 1.90, 1.95, 2.00, and 2.05 g/cm³ at 550 K.

the simulations and the experimental results. It should be noted that there are some experimental issues that need to be further investigated. As Franzese *et al.* [54] discussed, the density anomalies will occur if the slope of the liquid-liquid two-phase boundary is negative, as in water, but not if the slope of the two-phase boundary is positive. In the experiments of Henry *et al.* [36], the slope of the two-phase boundary is positive, but their experimental results show obvious density anomalies in both LDL and HDL. For example, as shown in Fig. 7(a), at about 0.5 GPa, the density at 845 K is obviously higher than at 740 K, indicating an anomalous temperature-dependent behavior. In addition, Henry *et al.* plotted some lines to highlight the discontinuous changes in density. However, if these lines are extended towards high and low pressures [as shown by the dashed lines in Fig. 7(a)], both HDL and LDL exhibit an anomalous dependence of density on temperature. For HDL, at pressures greater than 1.0 GPa, the density at 650 K will be lower than at 740, 845, and 950 K, and at pressures higher than 2.0 GPa, the density at 950 K will be lower than at 1035 K. For LDL, at pressures below 0.25 GPa, the density at 650 K will be larger than at 550 K. These temperature-dependent density anomalies are puzzling since no such anomaly has been observed in existing density measurements at low pressures. It should be noticed that, within the margin of error, the eye guide lines of the experimental data can also be drawn to the style as shown in Fig. 7(c). This may clear up the above puzzle, but implies that liquid sulfur is not undergoing a first-order phase transition.

Whether this is the case needs to be further verified by experimentally measuring more densities.

IV. CONCLUSION

DFT-based *ab initio* molecular dynamics simulations are used to investigate the experimentally observed first-order LLPT in molten sulfur. Our calculated pair correlation functions are in good agreement with the experimental results, and our simulations capture the structural changes between LDL and HDL. By studying the microstructure, we find that this structural change from LDL to HDL is actually a transition between two polymer phases with different degrees of order, with HDL having a higher degree of order than LDL. There are more S₈ diradical structures in the long chain of LDL, but less in the long chain of HDL. This structural change may be related to the self-organized behavior of long-chain molecules in molten sulfur. However, no discontinuous change in density is found along our simulated isotherms, that is, the structural change based on *ab initio* calculations is continuous but not a first-order LLPT. *Ab initio* molecular dynamics simulations give no evidence for a first-order LLPT.

ACKNOWLEDGMENTS

This work was supported by the National Natural Science Foundation of China (Grant No. 11874191) and the Natural

Science Foundation of Shandong Province of China (Grant No. ZR2019MA066). We acknowledge the Supercomputer

Center of Ludong University for providing computing facilities.

- [1] V. V. Brazhkin, R. N. Voloshin, and S. V. Popova, Nonmetal-metal transition in liquid Se under high pressure, *High Press. Res.* **4**, 348 (1990).
- [2] P. H. Poole, F. Sciortino, U. Essmann, and H. E. Stanley, Phase behaviour of metastable water, *Nature (London)* **360**, 324 (1992).
- [3] P. Gallo, K. Amann-Winkel, C. A. Angell, M. A. Anisimov, F. Caupin, C. Chakravarty, E. Lascaris, T. Loerting, A. Z. Panagiotopoulos, J. Russo, J. A. Sellberg, H. E. Stanley, H. Tanaka, C. Vega, L. Xu, and L. G. M. Pettersson, Water: A tale of two liquids, *Chem. Rev.* **116**, 7463 (2016).
- [4] S. Aasland and P. F. McMillan, Density-driven liquid-liquid phase separation in the system $\text{Al}_2\text{O}_3\text{-Y}_2\text{O}_3$, *Nature (London)* **369**, 633 (1994).
- [5] M. Togaya, Pressure dependences of the melting temperature of graphite and the electrical resistivity of liquid carbon, *Phys. Rev. Lett.* **79**, 2474 (1997).
- [6] J. N. Glosli and F. H. Ree, Liquid-liquid phase transformation in carbon, *Phys. Rev. Lett.* **82**, 4659 (1999).
- [7] Y. Katayama, T. Mizutani, W. Utsumi, O. Shimomura, M. Yamakata, and K. Funakoshi, A first-order liquid-liquid phase transition in phosphorus, *Nature (London)* **403**, 170 (2000).
- [8] Y. Katayama, Y. Inamura, T. Mizutani, M. Yamakata, W. Utsumi, and O. Shimomura, Macroscopic separation of dense fluid phase and liquid phase of phosphorus, *Science* **306**, 848 (2004).
- [9] G. Zhao, H. Wang, D. M. Hu, M. C. Ding, X. G. Zhao, and J. L. Yan, Anomalous phase behavior of first-order fluid-liquid phase transition in phosphorus, *J. Chem. Phys.* **147**, 204501 (2017).
- [10] H. Tanaka, R. Kurita, and H. Mataka, Liquid-liquid transition in the molecular liquid triphenyl phosphite, *Phys. Rev. Lett.* **92**, 025701 (2004).
- [11] G. Zhao, H. F. Mu, X. M. Tan, M. S. Wang, D. H. Wang, and C. L. Yang, First-order liquid-liquid phase transition in AsS melt caused by change of intermediate-range order, *J. Non-Cryst. Solids* **404**, 135 (2014).
- [12] V. V. Brazhkin, Y. Katayama, M. V. Kondrin, T. Hattori, A. G. Lyapin, and H. Saitoh, AsS melt under pressure: One substance, three liquids, *Phys. Rev. Lett.* **100**, 145701 (2008).
- [13] V. V. Brazhkin, M. Kanzaki, K.-i. Funakoshi, and Y. Katayama, Viscosity behavior spanning four orders of magnitude in As-S melts under high pressure, *Phys. Rev. Lett.* **102**, 115901 (2009).
- [14] S. Sastry and C. A. Angell, Liquid-liquid phase transition in supercooled silicon, *Nat. Mater.* **2**, 739 (2003).
- [15] N. Jakse and A. Pasturel, Liquid-liquid phase transformation in silicon: Evidence from first-principles molecular dynamics simulations, *Phys. Rev. Lett.* **99**, 205702 (2007).
- [16] P. Ganesh and M. Widom, Liquid-liquid transition in supercooled silicon determined by first-principles simulation, *Phys. Rev. Lett.* **102**, 075701 (2009).
- [17] V. V. Vasisht, S. Saw, and S. Sastry, Liquid-liquid critical point in supercooled silicon, *Nat. Phys.* **7**, 549 (2011).
- [18] G. Zhao, Y. J. Yu, and X. M. Tan, Nature of the first-order liquid-liquid phase transition in supercooled silicon, *J. Chem. Phys.* **143**, 054508 (2015).
- [19] G. Zhao, Y. J. Yu, J. L. Yan, M. C. Ding, X. G. Zhao, and H. Y. Wang, Phase behavior of metastable liquid silicon at negative pressure: *Ab initio* molecular dynamics, *Phys. Rev. B* **93**, 140203(R) (2016).
- [20] B. Boates and S. A. Bonev, First-order liquid-liquid phase transition in compressed nitrogen, *Phys. Rev. Lett.* **102**, 015701 (2009).
- [21] S. Scandolo, Liquid-liquid phase transition in compressed hydrogen from first-principles simulations, *Proc. Natl. Acad. Sci. USA* **100**, 3051 (2003).
- [22] M. A. Morales, C. Pierleoni, E. Schwegler, and D. M. Ceperley, Evidence for a first order liquid-liquid transition in high pressure hydrogen from *ab-initio* simulations, *Proc. Natl. Acad. Sci. USA* **107**, 12799 (2010).
- [23] V. Dzyabura, M. Zaghoo, and I. F. Silvera, Evidence of a liquid-liquid phase transition in hot dense hydrogen, *Proc. Natl. Acad. Sci. USA* **110**, 8040 (2013).
- [24] V. V. Brazhkin, I. Farnan, K.-i. Funakoshi, M. Kanzaki, Y. Katayama, A. G. Lyapin, and H. Saitoh, Structural transformations and anomalous viscosity in the B_2O_3 melt under high pressure, *Phys. Rev. Lett.* **105**, 115701 (2010).
- [25] G. Carini, Jr., A. Bartolotta, G. Di Marco, B. Fazio, M. Federico, V. Romano, G. Carini, and G. D'Angelo, Polyamorphism and liquid-liquid phase transition in B_2O_3 , *Phys. Rev. B* **105**, 014105 (2022).
- [26] V. V. Brazhkin, S. V. Popova, and R. N. Voloshin, High-pressure transformations in simple melts, *High Press. Res.* **15**, 267 (1997).
- [27] V. V. Brazhkin and A. G. Lyapin, High-pressure phase transformations in liquids and amorphous solids, *J. Phys.: Condens. Matter* **15**, 6059 (2003).
- [28] J. R. Morris, C. Z. Wang, and K. M. Ho, Relationship between structure and conductivity in liquid carbon, *Phys. Rev. B* **52**, 4138 (1995).
- [29] C. J. Wu, J. N. Glosli, G. Galli, and F. H. Ree, Liquid-liquid phase transition in elemental carbon: A first-principles investigation, *Phys. Rev. Lett.* **89**, 135701 (2002).
- [30] L. K. Templeton, D. H. Templeton, and A. Zalkin, Crystal structure of monoclinic sulfur, *Inorg. Chem.* **15**, 1999 (1976).
- [31] W. A. Crichton, G. B. M. Vaughan, and M. Mezouar, In situ structure solution of helical sulphur at 3 GPa and 400 °C, *Z. Kristallogr.* **216**, 417 (2001).
- [32] G. E. Sauer and L. B. Borst, Lambda transition in liquid sulfur, *Science* **158**, 1567 (1967).
- [33] L. Liu, Y. Kono, C. Kenney-Benson, W. Yang, Y. Bi, and G. Shen, Chain breakage in liquid sulfur at high pressures and high temperatures, *Phys. Rev. B* **89**, 174201 (2014).
- [34] G. Zhao and H. F. Mu, Pressure dependence of structural and dynamical properties in melt sulfur: Evidence for two successive chain breakages, *Chem. Phys. Lett.* **616-617**, 131 (2014).

- [35] D. Plašienka, P. Cifra, and R. Martoňák, Structural transformation between long and short-chain form of liquid sulfur from *ab initio* molecular dynamics, *J. Chem. Phys.* **142**, 154502 (2015).
- [36] L. Henry, M. Mezouar, G. Garbarino, D. Sifré, G. Weck, and F. Datchi, Liquid-liquid transition and critical point in sulfur, *Nature (London)* **584**, 382 (2020).
- [37] G. Kresse and J. Hafner, *Ab initio* molecular dynamics for liquid metals, *Phys. Rev. B* **47**, 558 (1993).
- [38] G. Kresse and J. Furthmüller, Efficient iterative schemes for *ab initio* total-energy calculations using a plane-wave basis set, *Phys. Rev. B* **54**, 11169 (1996).
- [39] P. E. Blöchl, Projector augmented-wave method, *Phys. Rev. B* **50**, 17953 (1994).
- [40] G. Kresse and D. Joubert, From ultrasoft pseudopotentials to the projector augmented-wave method, *Phys. Rev. B* **59**, 1758 (1999).
- [41] J. P. Perdew, K. Burke, and M. Ernzerhof, Generalized gradient approximation made simple, *Phys. Rev. Lett.* **77**, 3865 (1996).
- [42] J. P. Perdew and A. Zunger, Self-interaction correction to density-functional approximations for many-electron systems, *Phys. Rev. B* **23**, 5048 (1981).
- [43] R. Winter, P. A. Egelstaff, W. C. Pilgrim, and W. S. Howells, The structural properties of liquid, solid and amorphous sulphur, *J. Phys.: Condens. Matter* **2**, SA215 (1990).
- [44] See Supplemental Material at <http://link.aps.org/supplemental/10.1103/PhysRevB.109.014209> for convergence tests and comparative evaluations of different functionals. It also contains Refs. [35,43,45,46].
- [45] F. Fehér and E. Hellwig, Beiträge zur Chemie des Schwefels, 45. Zur Kenntnis des flüssigen Schwefels. (Dichte, Ausdehnungskoeffizient und Kompressibilität), *Z. Anorg. Allg. Chem.* **294**, 63 (1958).
- [46] K. Funakoshi and A. Nozawa, Development of a method for measuring the density of liquid sulfur at high pressures using the falling-sphere technique, *Rev. Sci. Instrum.* **83**, 103908 (2012).
- [47] S. Nosé, A unified formulation of the constant temperature molecular dynamics methods, *J. Chem. Phys.* **81**, 511 (1984).
- [48] R. Bellissent, L. Descotes, F. Boué, and P. Pfeuty, Liquid sulfur: Local-order evidence of a polymerization transition, *Phys. Rev. B* **41**, 2135 (1990).
- [49] K. S. Vahvaselka and J. M. Mangs, X-ray diffraction study of liquid sulfur, *Phys. Scr.* **38**, 737 (1988).
- [50] J. Sun, A. Ruzsinszky, and J. P. Perdew, Strongly constrained and appropriately normed semilocal density functional, *Phys. Rev. Lett.* **115**, 036402 (2015).
- [51] J. Sun, R. C. Remsing, Y. Zhang, Z. Sun, A. Ruzsinszky, H. Peng, Z. Yang, A. Paul, U. Waghmare, X. Wu, M. L. Klein, and J. P. Perdew, Accurate first-principles structures and energies of diversely bonded systems from an efficient density functional, *Nat. Chem.* **8**, 831 (2016).
- [52] A. Baranyai and D. J. Evans, Direct entropy calculation from computer simulation of liquids, *Phys. Rev. A* **40**, 3817 (1989).
- [53] A. Baranyai and D. J. Evans, Three-particle contribution to the configurational entropy of simple fluids, *Phys. Rev. A* **42**, 849 (1990).
- [54] G. Franzese, G. Malescio, A. Skibinsky, S. V. Buldyrev, and H. Eugene Stanley, Generic mechanism for generating a liquid-liquid phase transition, *Nature (London)* **409**, 692 (2001).